

Motion Control Strategy of Industrial Direct Drive Robot for Vibration Suppression*

Liangsong Huang

Shenyang Institute of Automation,
Chinese Academy of Sciences
Graduate School of Chinese Academy of Sciences
Shenyang, China
huangls@sia.cn

Daokui Qu, Fang Xu

Shenyang Institute of Automation,
Chinese Academy of Sciences
SIASUN Robot & Automation Co., Ltd
Shenyang, China
dkqu@sia.cn, xufang@siasun.com

Abstract - Although it has many advantages such as high mechanical rigidity, fast dynamic response and high efficiency and precision, a direct drive robot is easy to vibrate because of sensibility to non-linearity, variety of parameter and external disturbance. This paper presents a model correction control strategy, which corrects the unmodeled dynamics of control system and suppresses disturbances by a unique control structure with a state observer and a digital low-pass filter. Theoretical and experimental results indicate that this strategy can effectively eliminate high order dynamic, nonlinearity, measurement noise and variation of load torque in the control system, and improves a direct drive robot motion control system's stability, robustness and resistance to disturbances, effectively suppresses the vibration.

Index Terms - direct drive robot, model correction, Motion Control, Vibration Suppression.

I. INTRODUCTION

In recent years, industrial direct drive robots have an increased application in semiconductor manufacturing systems or numerical control machine systems which need high-performance and high-precision motion control technologies. Direct drive robot is driven by direct drive motor whose output shaft connects the arm of robot directly, eliminating problems associated with gearboxes and belts such as backlash, frictions, low stiffness, and complex mechanical structure, hence improving the overall performance of motion control of robot with its advantageous features of efficiency, high speed, high precision, fast response, low noise^[1].

However, the absence of the auxiliary mechanisms increases the sensitivity of the robot to uncertainties, the lump of uncertainties is usually composed of torque ripples, parameter variations, external disturbances, self non-linearity, and unmodeled dynamics, leading the direct drive robot moves and orients easily with vibration.

In view of these problems, the traditional linear controllers can't provide good control performance for the direct drive robot, state feedback adaptive control^[2], adaptive fuzzy sliding mode control^[3], learning neuro-fuzzy control^[4], integral variable structure control^[5-8] have been proposed to handle such problems. However, although those methods can improve its robustness to some extent, their designing

processes are complicated, and industrial reliabilities and applicabilities are poor. For the technical features of direct drive robot motion control, this paper presents a model correction control strategy, which corrects the unmodeled dynamics of control system and suppresses disturbances by a unique control structure with a state observer and a digital low-pass filter, effectively suppressing the vibration and giving full pay to the advantages of directive drive robot motion control.

II. PRINCIPLE OF MODEL CORRECTION CONTROL

Low-order linear system is the most typical system for analysing control theories and implementing control strategies, the direct drive robot motion control system which is a high-order nonlinear system is often simplified approximately as second-order linear system. However, if higher order dynamics and nonlinearity can't be rejected by simplification, they will rather destroy the control system's dynamic property and stability, therefore, this paper proposes a unique control strategy, which corrects high-order nonlinear system to second-order linear system to eliminate higher order dynamics and nonlinearity, the schematic diagram is shown in Fig. 1.

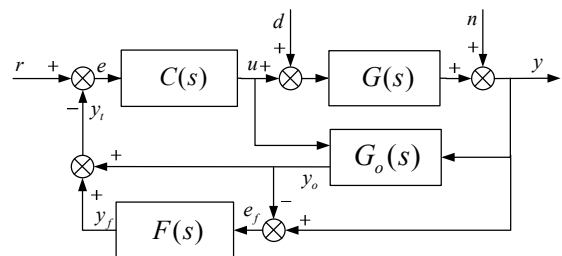


Fig. 1 Schematic diagram of model correction control.

As shown in Fig. 1, $G(s)$ denotes the controlled object, $C(s)$ is the controller, $G_o(s)$ is the state observer, $F(s)$ refers to the low-pass filter, d is the external disturbance, n stands for measurement noise. The output of the plant $y(s)$ can be decomposed as follows:

$$y(s) = y_d(s) + y_n(s) \quad (1)$$

* This work is partially supported by Important National Science & Technology Specific Projects under contract No.2009ZX02012.

where $y_d(s)$ refers to the component of plant output which corresponds to the dominant (second-order) dynamics, and $y_n(s)$ represents the components of the plant output which correspond to the higher order dynamics and noise. The output of the state observer can be also decomposed in the following form:

$$y_o(s) = y_{od}(s) + y_e(s) \quad (2)$$

where $y_{od}(s)$ is the component of state observer output which corresponds to the dominant dynamics, $y_e(s)$ represents the state observer estimation error, then assuming

$$y_d(s) \cong y_{od}(s) \quad (3)$$

the input of low-pass filter $F(s)$ in Fig 1 is

$$\begin{aligned} e_f(s) &= y(s) - y_o(s) = y_d(s) + y_h(s) - y_{od}(s) - y_e(s) \\ &= y_h(s) - y_e(s) \end{aligned} \quad (4)$$

the output of low-pass filter is

$$y_f(s) = F(s)[y_h(s) - y_e(s)] = F(s)y_h(s) - F(s)y_e(s) \quad (5)$$

because the low-pass filter is designed to attenuate the undesirable frequency components corresponding to the higher order dynamics and noise, $y_h(s)$ is virtually eliminated from the signal. In contrast, the state observer estimation error $y_e(s)$, being of low-frequency nature, passes through ideally, so

$$y_f(s) = -y_e(s) \quad (6)$$

Finally the feedback signal corrected is given by

$$y_t(s) = y_o(s) + y_f(s) = y_{od}(s) + y_e(s) + y_f(s) = y_{od}(s) \quad (7)$$

as shown in (7), the feedback signal is the output response of the dominant dynamics component of the plant, rejecting effects of undesirable higher order dynamics, measurement noises, and unmodeled error, to avoid deteriorating control performance due to amplitude and phase distortion of the feedback signals which are caused by implementation of low-pass and band-reject filters.

III. DESIGN OF ROBOT MOTION CONTROL SYSTEM

A. Robot Correction Control Strategy

According to the principle of model correction control, a detailed block diagram of the direct drive robot model correction control is presented in Fig. 2.

In the figure, $\theta_{r1,2}$, $\dot{\theta}_{r1,2}$, $\ddot{\theta}_{r1,2}$ denote the commanded trajectory converted to angular position, angular speed, angular acceleration of the motors 1 and 2, $\tau_{1,2}$ are torques exerted by the motors, $\theta_{1,2}$ stand for angular obtained from the encoders, $\dot{\theta}_{o1,2}$ are the outputs of state observer, $\dot{\theta}_{c1,2}$ are the output of low-pass filter, $\dot{\theta}_{s1,2}$ are the feedback signals, $v_{1,2}$ are the inputs of state observer.

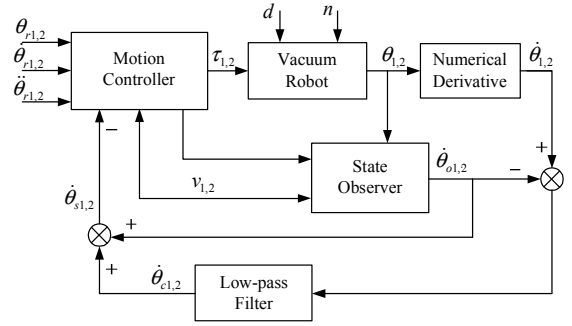


Fig. 2 Schematic diagram of direct drive robot model correction control.

B. Design of Motion Controller

The motion controller of direct drive robot motion control system alone operates based on position and velocity feedback using a standard implementation of the computed torque technique. The control law comprises a proportional-derivative(PD) compensator and a disturbance observer for each of the motors. The disturbance observers are used in place of conventional integrators for improved tracking performance and prompt elimination of steady state errors. A complete block diagram of the controller is provided in Fig. 3.

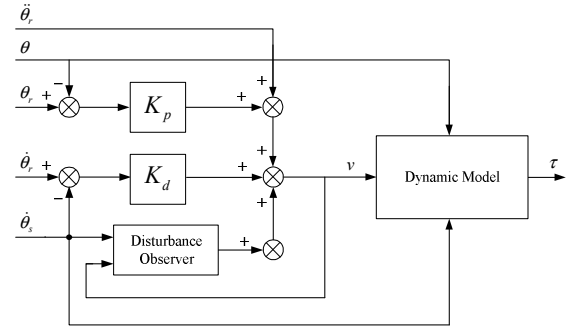


Fig. 3 Schematic diagram of direct drive robot motion controller.

The control law of motion controller is represented by the dynamic model block in Fig. 3. The control torques of robot are produced according to the following equations:

$$\begin{aligned} \tau_1 &= M_{11}(\theta_1, \theta_2)v_1 + M_{12}(\theta_1, \theta_2)v_2 + D_{111}(\theta_1, \theta_2)\dot{\theta}_{s1}^2 \\ &\quad + D_{122}(\theta_1, \theta_2)\dot{\theta}_{s2}^2 + D_{112}(\theta_1, \theta_2)\dot{\theta}_{s1}\dot{\theta}_{s2} \end{aligned} \quad (8)$$

$$\begin{aligned} \tau_2 &= M_{21}(\theta_1, \theta_2)v_1 + M_{22}(\theta_1, \theta_2)v_2 + D_{211}(\theta_1, \theta_2)\dot{\theta}_{s1}^2 \\ &\quad + D_{222}(\theta_1, \theta_2)\dot{\theta}_{s2}^2 + D_{212}(\theta_1, \theta_2)\dot{\theta}_{s1}\dot{\theta}_{s2} \end{aligned} \quad (9)$$

where v_1 represents the combined output of the PD compensator and disturbance observer plus reference angular acceleration for motors 1, and v_2 denotes the same quantity for motor 2. M_{11} and M_{22} are respectively effective inertia of each joint, M_{12} and M_{21} are respectively coupling inertia of each joint, D_{111} , D_{122} , D_{211} and D_{222} are coefficients of centripetal, D_{112} and D_{212} are coefficients of Coriolis.

While the position measurements are fed back to the controller directly from the encoders, synthetic velocity signals obtained from the combination of state observer and low-pass filter as indicated in Fig.3. This hybrid

implementation is selected since it is primarily the derivative section of the controller which amplifies the higher frequency components of the velocity signals corresponding to the undesirable vibration modes and measurement noise. The raw velocity signals are obtained by numerical differentiation of the encoder readings.

The state observer is employed to track the rigid-body dynamics of the robotic manipulator within a specified bandwidth. Because the control law reduces the rigid-body dynamics of the robot to a pair of independent unit inertia moments, it is convenient to partition the state observer into two identical sections designed for a simple single degree of freedom system. Each of the sections operates based on the following state equation:

$$\begin{bmatrix} \dot{x}_{i1} \\ \dot{x}_{i2} \end{bmatrix} = \begin{bmatrix} -2\zeta_o\omega_o & 1 \\ -\omega_o^2 & 0 \end{bmatrix} \begin{bmatrix} x_{i1} \\ x_{i2} \end{bmatrix} + \begin{bmatrix} 2\zeta_o\omega_o & 0 \\ \omega_o^2 & 1 \end{bmatrix} \begin{bmatrix} \theta_i \\ v_i \end{bmatrix} \quad (10)$$

where x_{i1} and x_{i2} are observed states (angular and velocity) of motor i , and ω_o and ζ_o denote the natural frequency and damping ratio associated with the dynamics of the state observer.

The Low-pass filter of Fig. 3 comprises a pair of linear second-order low-pass filters, one for each motor. The filters are represented by the following transfer function:

$$G_c(s) = \omega_c / (s^2 + 2\zeta_c\omega_c s + \omega_c^2) \quad (11)$$

where ω_c is the cut-off frequency and ζ_c the damping ratio associated with the poles of the filter. The state observer and low-pass filter are converted to a discrete-time formulation using bilinear transformation.

IV. SIMULATION TESTS

In order to confirm the validity of the proposed strategy, the computer simulation were implemented for the control system model made up from Table I. Typical operations performed by the robot include radial moves and rotational moves. The performance of the model correction control strategy is tested for a simple straight-line move from initial radial position of 0.2m to final extension of 0.7m.

TABLE I
DYNAMIC PROPERTIES OF DIRECT DRIVE ROBOT

Length of link 1	0.25m
Length of link 2	0.25m
Length of link 3	0.36m
Mass of link 1	2.32 kg
Mass of link 2	1.69 kg
Mass of link 3	2.73 kg
Inertia of link 1 with respect to axis of rotation	$1.34 \times 10^{-3} \text{kgm}^2$
Inertia of link 2 with respect to axis of rotation	$1.74 \times 10^{-3} \text{kgm}^2$
Inertia of link 1 with respect to center of gravity	$3.45 \times 10^{-3} \text{kgm}^2$
Inertia of link 2 with respect to center of gravity	$2.25 \times 10^{-3} \text{kgm}^2$
Inertia of link 3 with respect to center of gravity	$1.99 \times 10^{-3} \text{kgm}^2$
Inertia of payload with respect to center of gravity	$0.29 \times 10^{-3} \text{kgm}^2$
Lowest natural frequency interfering	22Hz

The effects of the model correction control strategy in the velocity loop are shown in Fig. 4 and Fig. 5. We can see that the raw velocity signals are contaminated by undesirable high-frequency components (hairline). Conventionally, the signals would be passed through the low-pass filters, resulting in significant phase-lag distortion (dashed line), and the output of state observer comes about phase-ahead distortion (dotted line) because of the modeling, and the low-pass filters are employed merely to eliminate inevitable observation errors resulting from modeling imperfections. In this particular application, the observation errors can be attributed primarily to inaccuracy of the model parameters. Combining the observed velocities with the outputs of the low-pass filters yields clean synthetic signals which exclude undesirable high-frequency components (bold line). The signals show substantially smaller errors than the filtered and observed velocities alone.

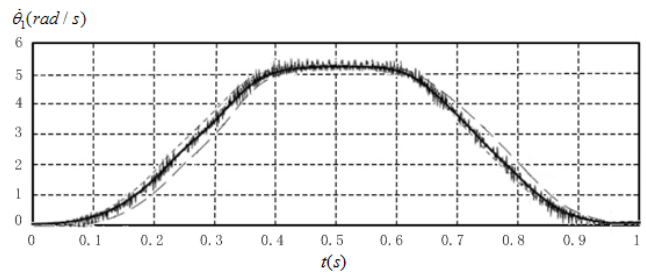


Fig. 4 Velocity profiles of motor 1.

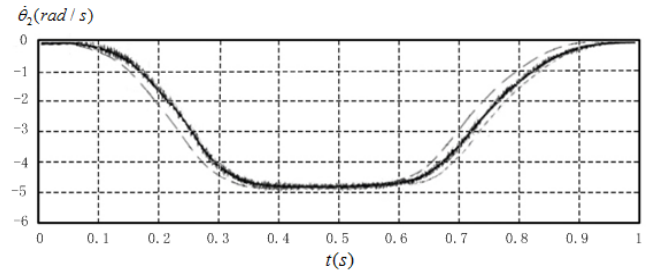


Fig. 5 Velocity profiles of motor 2.

In order to demonstrate the improvement due to the model correction control mechanism, the control performance is compared with an equivalent conventional control approach in terms of motor tracking errors. The state observer is disconnected in this case. The raw velocity signals are passed through the low-pass filters and fed back to the controller. The tracking errors are compared in Fig. 6 and Fig. 7. The graphs indicate that the tracking performance of the conventional control (hairline) is improved by an order of magnitude by implementing the model correction control mechanism (bold line).

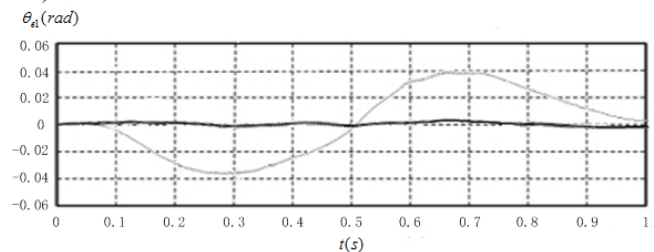


Fig. 6 Tracking errors of motor 1.

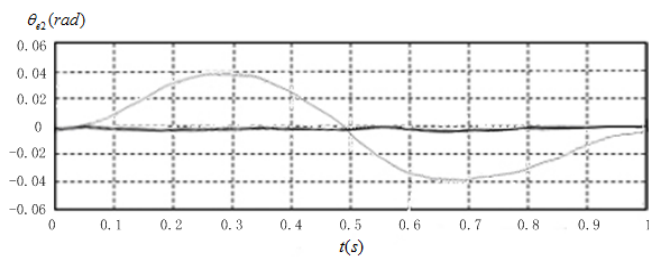


Fig. 7 Tracking errors of motor 2.

V. CONCLUSION

This paper proposed the model correction control strategy to deal with the problems of direct drive robot motion control that is sensible to the uncertainties in the drive system. This strategy designs a unique control structure with a state observer and a digital low-pass filter to eliminate high order dynamic, nonlinearity, high frequency noise and variation of load torque, effectively suppressing the vibration and improving the performance of direct drive robot motion control system. The effectiveness of the proposed concept is demonstrated theoretical analysis and simulation results.

ACKNOWLEDGMENT

This work has been financed by the Important National Science & Technology Specific Projects under contract No. 2009ZX02012.

REFERENCES

- [1] Kemalettin Erbatur, and Berk Calh, Fuzzy Boundary Layer as Applied to the Control of a Direct Drive Robot[J]. The 33rd Annual Conference of the IEEE Industrial Electronics Society, 2007, pp.2858-2863.
- [2] Kim YT, Akbarzadeh-T MR, Lee DW. State Feedback Adaptive Control of a Direct Drive Motor[J]. System Theory, 1997, Proceedings of the Twenty-Ninth Southeastern Symposium on, 1997:288-291.
- [3] Kim YT, Akbarzadeh-T. MR, Lee DW, Lee SR. Adaptive Fuzzy Sliding Mode Control of a Direct Drive Motor[J]. Systems, Man, and Cybernetics, 1997 'Computational Cybernetics and Simulation', 1997 IEEE International Conference on, 1997, 2(12):1668-1673.
- [4] Kumbala KK, Jamshidi M. Real time control of a direct drive motor by a learning neuro-fuzzy controller[J]. Systems, Man, and Cybernetics, 1997 'Computational Cybernetics and Simulation', 1997 IEEE International Conference on, 1997, 2(12):1674-1679.
- [5] Chung SK, Lee JH, Ko JS, Youn MJ. Robust speed control of brushless direct-drive motor using integral variable structure control[J]. Electric Power Applications, IEE Proceedings, 1995, 142(6):361-370.
- [6] Chung S-K, Lee J-H, Ko J-S, Youn M-J. A robust speed control of brushless direct drive motor using integral variable structure control with sliding mode observer[J]. Industry Applications Society Annual Meeting, 1994, Conference Record of the 1994 IEEE, 1994:393 - 400.
- [7] Zhu G, Dessaint L-A, Akhrif O, Kaddouri A. Speed tracking control of a permanent-magnet synchronous motor with state and load torque observer[J]. Industrial Electronics, IEEE Transactions on, 2000, 47(2):346-355.
- [8] Mohamed YA-RI. A Hybrid-Type Variable-Structure Instantaneous Torque Control With a Robust Adaptive Torque Observer for a High-Performance Direct-Drive PMSM[J]. Industrial Electronics, IEEE Transactions on, 2007, 54(5):2491-2499.